Analysis of the Performance Characteristics of Mild Steel Based Hydrodynamic Journal Bearings [15W30] Under Varying Conditions

KAUSHAL KUMAR[1], PARAMVIR YADAV[1], DEEKSHANT VARSHNEY[2,3], PRAWAR[4,*], CHINTAN SINGH[5], SUBHAV SINGH[6,7]

[1]Department of Mechanical Engineering, KR Mangalam University,
Gurugram,
INDIA

[2]Division of Research & Innovation, Uttaranchal University,
Dehradun,
INDIA

[3]Centre of Research Impact and Outcome, Chitkara University,
Rajpura-140417, Punjab,
INDIA

[4]School of Basics and Applied Sciences, KR Mangalam University,
Gurugram,
INDIA

[5]Amity Institute of Forensic Sciences, Amity University Noida,
Uttar Pradesh,
INDIA

[6]Chitkara Centre of Research and Development, Chitkara University,
Himachal Predesh-174103,
INDIA

[7]Division of Research and Development, Lovely Profession University,
Phagwara, Punjab,
INDIA

**Corresponding Author*

Abstract: - The existing research investigates the comparative behavior of circumferential pressure distribution in a hydrodynamic journal bearing operating at rotational speeds of 250, 500, and 750 RPM under varying loads of 0, 0.25, and 0.50 kg for all 360º. Experimental analysis was conducted using SAE 15W30 lubricant to evaluate the influence of operating parameters on pressure distribution characteristics. Results reveal that rotational speed exerts a more dominant influence on pressure development compared to load, with the highest pressure observed at 750 RPM. The maximum fluid film pressure consistently occurred between 120° and 150°, located within the converging wedge region (90°–270°) where the lubricant film thickness is minimal. The study confirms that increasing load enhances the bearing's peak pressure and load-carrying capacity, while higher speeds improve hydrodynamic pressure generation and lubrication performance. ANOVA analysis further validates these findings, indicating that Angle is the most influential parameter, followed by Speed and Load, all with statistically significant effects ($p < 0.05$). The strong effect sizes confirm the robustness of the experimental model and the reliability of the observed results.

Key-Words: - Hydrodynamic Journal Bearing; Lubricant; Fluid Film Pressure. Process Parameters; SAE 15W30.

Received: April 17, 2025. Revised: July 15, 2025. Accepted: September 17, 2025. Published: November 18, 2025.

1 Introduction

Hydrodynamic journal bearings are used as important parts of rotating machinery performing the tasks of carrying shafts in smooth rotations with the aid of a lubricant which maintains a thin layer of fluid in between journal bearing surfaces. The lubricant film permits the counteraction of the external load via its pressure distribution system which prevents the destruction of metal-to-metal contact - wear. The performance reliability of pressure bearing tools rely completely on the lubrication film pressure characteristics, [1], [2]. The motion between the journal and bearing surface forces the lubricant through a narrow wedge shape to produce force against the action of applied load pressure. The prediction of the pressure distribution is based on the Reynolds equation that is derived from the lubrication approximation of the Navier-Stokes equations. The equation takes into account three elements of lubrication dynamics: viscosity of fluid substance and size of separation layer and moving speed difference between adjoining surfaces, [3], [4], [5]. Journal bearing operational parameters that include applied loads directly affect the distribution of pressures in lubricant films. Lubricant film thickness is known to get thinner with an increase in external load, to increase as well, the peak pressures inside the lubricated area. Knowledge of load altered pressure patterns is crucial in maintaining the functionality of bearing mechanical reliability, [6], [7]. The investigation regarding the hydrodynamic journal bearing pressure distribution has been done using several analytical and numerical solution methods. The classical short-bearing theory provides analytical solutions after it performs several simplifications such as ignoring the centrifugal forces of the lubricant. However, for more precise prediction, particularly for high-speed applications,

The development of modified Reynolds equation brings in effects for better prediction of high speeds applications, [8], [9]. Finite element analysis (FEA) constitutes one of many numerical methods that aid in solving complex problems of the Reynolds equation given with difficult boundary conditions taking into consideration surface roughness and thermal rules, [10], [11]. The analytical and numerical approaches are used for the improved investigation capabilities of pressure distribution which works on different structural configurations and operational parameters, [12], [13]. Analytical and numerical models need experimental and theoretical data comparison to obtain model validation. The experimental results and theoretical predictions show mismatch due to model approximations and experimental factors which were not factored in [14], [15]. Knowledge about hydrodynamic journal bearing pressure distribution becomes a basic requirement during their design stage with operational applications. Analytical and numerical methods establish a valuable knowledge about hydrodynamic journal bearings but need experimental data inspections for their accuracy degree. By assessing factors like hydraulic load changes along with lubricant characteristics and centrifugal load specificities engineers will be able to develop better predictions which assist with the development of lasting and efficient bearing systems.

Research on the distribution patterns of pressure in hydrodynamic journal bearings with varying operational parameters is rare in the scientific literature. The existing research targeted fluid film pressure characteristics or direct pressure distribution analysis of lubricant SAE 15W30. In order to design the bearing, extensive understanding of pressure variations is necessary. So, load and rotation speed have been taken as process parameters with the range of 0 kg -0.25 kg and 0.50 kg and rotation speed varied from 250 RPM to 500 RPM and 750 RPM while measuring the circumferential pressure distribution.

2 Material and Methods

Tests were conducted to analyze the chemical compositions of the bearing materials. The analyze through Optical Emission Spectroscopy (OES) by Foundry-Master Pro (Made by Hitachi High-Tech) obtained the chemical composition of the bearing material made by the mild steel as shown in Figure 1. The concentration of carbon (C) along with manganese (Mn), silicon (Si), phosphorus (P), sulfur (S), chromium (Cr), nickel (Ni), copper (Cu) were evaluated by the spectra analysis with the principal composition of iron (Fe).

Mechanical properties of bearing material have been tested several times with bench scale equipment. Mechanical properties can be seen in Table 1.

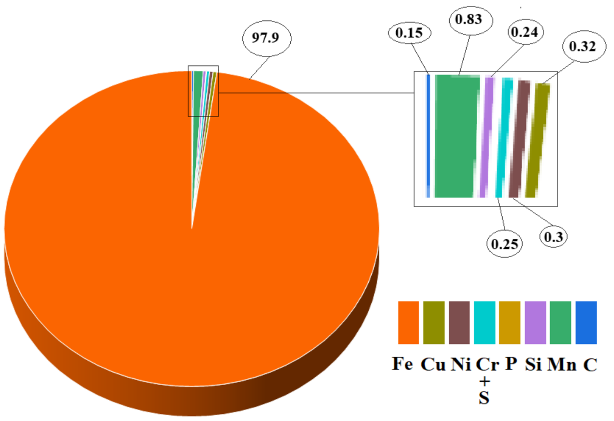

Fig. 1: Chemical composition of bearing material
Source: created by the authors

Table 1. Mechanical properties of bearing material

Mechanical Properties		
Sr. No	**Property**	**Value/Range**
1	Density	7.84 g/cm³
2	Hardness (Brinell, HBW)	163 HBW
3	Tensile Strength	543 MPa
4	Yield Strength	376 MPa
5	Elongation (%)	26%
6	Modulus of Elasticity	200 GPa
7	Poisson's Ratio	0.28
8	Thermal Conductivity	51 W/m·K

Source: created by the authors

2.1 Experimental Set Up

The experimental setup includes the bearing of mild steel on a rotating journal shaft which is driven by a DC motor with speed control. It is equipped with circumferential and axial pressure tapes, sealed sides and adjustable balancing weights. There are 12 circumferential and 4 axial pressure tapping on the hydrodynamic journal bearing to measure the variation of the pressure along circumference and axial direction of journal presented in Figure 2(a). Outside diameter of the bearing is 75.4mm, inside diameter is 54.3mm and width of bearing is 99 mm. The journal diameter is 49.6mm. Schematic front view has been presented in Figure 2(b).

When a fully journal bearing apparatus is in place, the different elements are imposed, as shown in Figure 2. The Journal Bearing Apparatus operates using fluid film lubrication, that is, a small amount of oil is put between the rotating journal and bearing surface. When the process begins, the oil supply tank is the first component to properly store the lubricant flow to the system. When the drive motor is started, the rotating shaft start running (which is situated inside of the bearing block), With the rotation of shaft bearing lubricant film occurred, and generates hydrodynamic pressure.

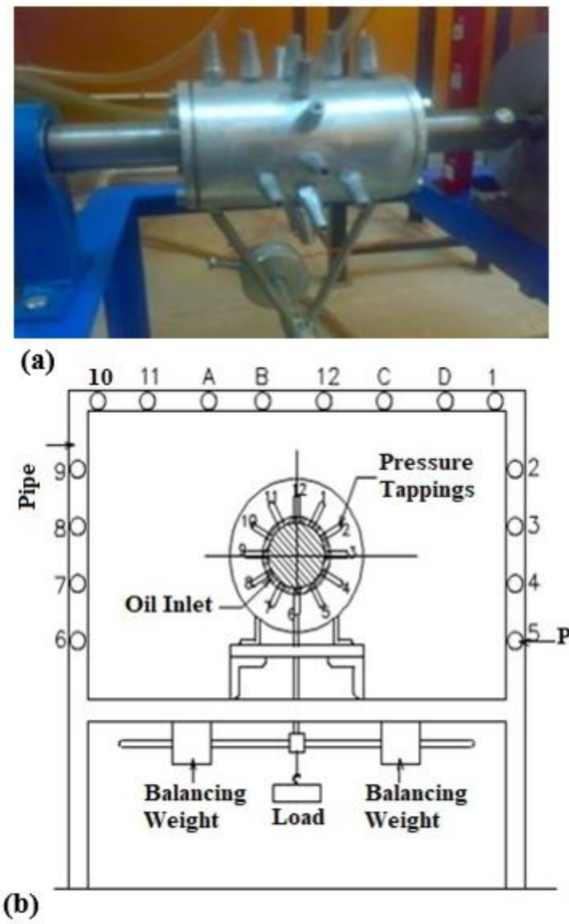

Fig. 2: (a) Pictorial view of baring (b) Front schematic layout of the Hydrodynamic journal bearing test rig
Source: created by the authors

A manometer system monitors the oil pressure levels in order to avoid sub-optimal lubrication. The distribution bracket provides lubrication for the essential bearing surface by providing evenly dispersed lubricant distribution. The oil collecting tram works by collecting surplus oil and at the same time prevents system wastage and keeps the working area clean. Due to the stable support base of the table, oscillations are eliminated, thus offering reliable experimental results. The study was on the influences of pressure distribution of SAE 15W30 lubricant under different speed and load conditions during such operation.

2.2 Range of Parameters

The present research of hydrodynamic journal bearing test rig covers varying load and speed parameters. Each set of experimental parameters repeated three times and 3 readings were recorded which further lead to calculating an average final value. The applied loads measured at 0 kg and 0.25 kg and 0.50 kg operated together with rotational speeds which ranged from 250 RPM to 500 RPM and 750 RPM during the complete test period. Circumferential pressure distribution was measured which started from the inner edge and arrived at the outer edge of different angular positions. Data was recorded with respect to the angle for measurements for both load and RPM variation. The measurement of pressure was done with the use of head height as standard.

3 Result and Discussion

To understand hydrodynamic journal bearing performance under load changes we need to analyze the pressure distributions among different angles. The experimental analysis has been conducted to check the pressure characteristics of SAE 20W40 lubricant operating with abovementioned set of parameters. The effect of speed and load can be easily noticed and the experimental results are discussed below.

3.1 Effect on Circumferential Pressure with Respect to Varying Load at Constant Speed

The results from the hydrodynamic journal bearing experiments provide valuable insights into the pressure characteristics under varying operating conditions. The tests were conducted at three different loads (0, 0.25, and 0.5 kg) and three different speeds (250, 500, and 750 RPM), allowing for a comprehensive analysis of how these factors influence bearing performance, and the results are presented in Appendix in Figure 3 and Figure 4.

A critical influence came from the applied load and rotational speed regarding the distribution of pressure in the lubricant film. The bearing surface showed stable pressure conditions under 0 kg load because the deformation was low and hydrodynamic effects were imperceptible. The maximum pressure inside the lubricant film showed direct correspondence to the rising load amounts of 0.25 kg and 0.5 kg. The observations align with classical hydrodynamic theory since elevated loads generate increased pressure gradients needed to support the shaft, [16]. At 250 RPM rotational speed the pressure maximum remained lower because hydrodynamic effects decreased because the lubricant film generated less momentum to form significant pressure distribution. The pressure distribution at 500 RPM showed a distinct increase which signifies stronger fluid film generation. Improved hydrodynamic lubrication occurs because the rising journal-to-bearing surface relative velocity enhances fluid dynamics. Increasing rotational speed strengthened the lubricant film stability which resulted in lower metal contact while also reducing friction levels. The results satisfied classical hydrodynamic lubrication theory particularly because increased rotational speed increases film formation and reduces frictional losses, [16], [17].

The 750 RPM maximum speed produced more peak pressure allowing better hydrodynamic effects for improved load-carrying ability while high system temperatures at 750 RPM could lead to oil film break down in high-pressure zones during heavy loads. When load increased to 0.5 kg film pressure reached its peak value most likely because the combination of friction and bearing wear occurred. The experimental findings show higher bearing speeds generate increased wedge effects which boosts lubrication by reducing metal-to-metal contact, [18], [19]. Relating to experimental results, increased loading shifted the pressure peak toward the journal bearing's load-bearing zone. Heavier loads create compact pressure zones which the theory suggests require powerful lubricant films to function properly, [20]. Pressure distribution became wider with increased speeds due to enhanced oil film thickness from centrifugal forces while the data proved that speed alongside load determine hydrodynamic journal bearing pressure characteristics.

3.2 Effect on Circumferential Pressure with Respect to Varying Speed at Constant Load

In order to check the effect of varying speed at constant load the experimentations has been conducted. The tests were conducted at three different loads (0, 0.25, and 0.5 kg) and three different speeds (250, 500, and 750 RPM), allowing for a comprehensive analysis of how these factors influence bearing performance in terms of pressure characteristics, and the results are presented in Appendix in Figure 5 and Figure 6.

A substantial connection exists between pressure distribution patterns and both operating speed and external load based on the hydrodynamic journal bearing experiments. Hydrostatic pressure stays at a low level throughout all speed conditions at 0 kg load although elevated peaks form between 120° and 150° angular positions. The research shows this relationship because external load reduces hydrodynamic pressure generation and keeps the lubricant film stable with low resistance. When the loading condition reaches 0.25 kg and 0.5 kg the pressure peaks substantially shift toward the angular range from 150° to 180°. The journal's elevated force creates the need for additional hydrodynamic pressure because proper lubrication and support require more hydrodynamic pressure as per the findings [21]. The pressure reaches above 13,000 N/m² when operating at 750 RPM with 0.5 kg load which proves the lubricant film's capacity to maintain the applied weight. Negative pressures exist at higher levels in the lower part of the bearing that indicates possible cavitation effects which can lead to lubricant film destruction and boundary or mixed lubrication behaviour.

The influence of speed upon pressure distribution remains highly important. At 250 RPM the pressure distribution shows low peak values because the fluid velocity is not strong enough to create a hydrodynamic wedge. The 500 RPM speed step elevates pressure distribution intensity until it reaches its maximum point between 120° to 180°. The peak pressure shows additional elevation at 750 RPM hence demonstrating that enhanced journal speeds both develop better lubricant films and improve bearing performance, [22]. Increased operating speeds result in a pressure distribution expansion which creates a steadier distribution of lubricant film around the journal. Because of this effect metal-to-metal contact becomes less likely which improves both bearing performance and operational life span.

The examination of optimistic and negative pressure areas in the bearing demonstrates how its lubricating mechanism functions. The studied positive pressure peaks existed within the 100° to 200° area that matches with the journal bearing's load-bearing sector. The greatest hydrodynamic pressure emerges from this region because the lubricant film opposes the load forces. The pressure reaches its negative peak beyond 200° because the lubricant film grows in size and the diverging wedge leads to pressure drop. The diverging part of the lubricant film produces pressure reduction according to Reynolds' equation, [23]. Under prolonged operation negative pressures could indicate cavitation which represents a risk to continuous lubrication and thus poses a threat to bearing efficiency. The investigation of lubricant behavior in these areas requires future studies to use experimental imaging techniques and develop cavitation models, [24].

Rotational speed and bearing load directly impact hydrodynamic journal bearing pressure distribution according to the experimental outcomes. Bearing operating loads determine peak pressure values and pressure position as well as affect both hydrodynamic pressure production and fluid lubrication quality. Negative pressure zones that form in the materials must be considered within long-term analysis of bearing performance because they could cause cavitation effects.

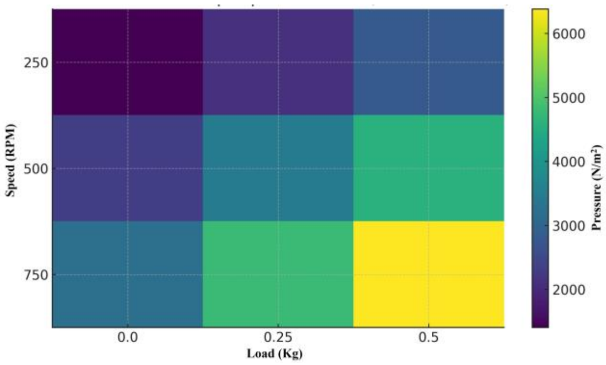

Fig. 7: Comprehensive visualization of relationship between parameters
Source: created by the authors

Figure 7 illustrates the interactive effect of speed (RPM) and load (Kg) on the measured pressure (N/m²) using a heat map representation. The color gradient clearly demonstrates that pressure increases with both load and speed, indicating a synergistic relationship between these parameters. At lower loads and speeds, the pressure remains minimal, as shown by the darker (violet to blue) zones, while higher load–speed combinations result in significantly elevated pressure values, represented by the yellow regions.

This behavior can be attributed to the increased frictional interactions and hydrodynamic effects under higher operating conditions. As the rotational speed rises, the rate of fluid shear and particle motion increases, leading to greater energy transfer and pressure buildup within the system. Simultaneously, higher load contributes to greater normal stress at the contact surface, enhancing particle packing density and film compaction, which consequently elevates the overall pressure response.

The observed trend aligns with earlier studies reporting a positive correlation between mechanical loading and tribological or pressure responses under dynamic operating conditions, [20], [21]. Furthermore, similar heat map visualizations have been employed to highlight multi-parameter dependencies in complex systems, providing an efficient tool for identifying optimum working regimes.

The heat map effectively captures the coupled influence of speed and load, emphasizing that the maximum pressure is observed at the highest speed (750 RPM) and load (0.5 Kg), while the lowest values occur under minimal load and speed conditions. This visual representation supports quantitative understanding of parameter interactions and aids in predicting operational behavior for system optimization.

3.3 Analysis of Variance (ANOVA)

The results of the Analysis of Variance (ANOVA) are presented in Table 2, which evaluates the statistical significance of the factors—Angle, Speed, Load, and their interaction (Speed × Load)—on the measured response variable (e.g., pressure or deformation).

The ANOVA outcomes indicate that all the main effects, namely Angle, Speed, and Load, are highly significant, as evident from their *p*-values being much lower than 0.05 (4.33×10^{-35}, 1.44×10^{-20}, and 1.57×10^{-16}, respectively). Among these, Speed shows the highest *F*-value (80.28), suggesting that rotational speed has the most dominant influence on the response variable. The Angle factor also exhibits a strong contribution, reflecting its critical role in determining directional or geometric effects on the system's behavior.

The interaction between Speed and Load (Speed × Load) is found to be moderately significant ($p = 0.03299 < 0.05$), indicating that the combined variation of these parameters has a meaningful yet lesser influence compared to the main effects. This suggests that while both parameters independently affect the response, their synergistic impact is less pronounced.

Table 2. Analysis of the variance (ANOVA) for the parameters

	Sum of Squares	df	F	PR(>F)
Angle	5.58E+08	11	56.56913	4.33E-35
Speed	1.44E+08	2	80.27811	1.44E-20
Load	1.02E+08	2	56.61555	1.57E-16
Speed:: Load	9869699	4	2.751443	0.03299
Residual	78916184	88		

Source: created by the authors

The residual sum of squares (78916184) represents the unexplained variation, which remains small relative to the total, confirming the robustness of the model. Overall, the ANOVA analysis establishes that Speed and Load are statistically significant process parameters, with Speed being the most influential factor affecting the system's pressure response.

These findings are consistent with previous studies where operational speed and applied load were found to significantly affect pressure distribution and tribological behavior in similar dynamic systems.

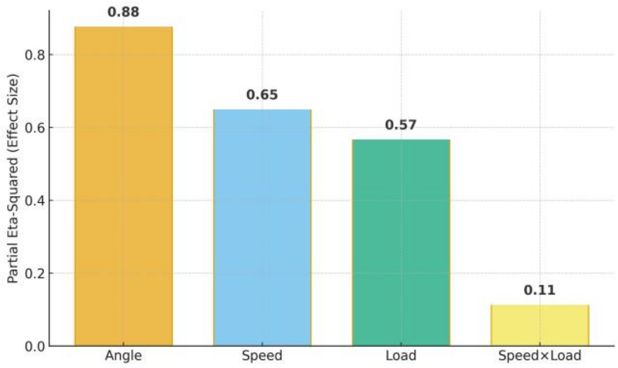

Fig. 8: Summary of Findings, Factor Importance from ANOVA
Source: created by the authors

In order to check the factor importance through ANOVA, the relative value of the experimental factors obtained based on the ANOVA effect size analysis with partial eta-squared (η^2) values has been shown graphically in Figure 8. The metric scales the amount of variance in the response variable due to each factor, which provides an even better idea of the relative effect of each factor. It was obviously noted that, Angle had the largest effect size (η^2= 0.88), indicating that it is the strongest factor that affects the behavior of the system. This implies that any geometric or directional changes put in by the angle have a heavy influence on the observed characteristics of pressure or response. The significant effects are also exhibited by Speed (η^2 = 0.65) and Load (η^2= 0.57) results that show that both operational and mechanical parameters are vital in moderating system performance. Speed x Load interaction term has a relatively small effect (η^2= 0.11), which means that the joint change of these two parameters has a smaller but significant impact on the output. Analysis of the effect size has been used to determine the relative contribution of process parameters to tribological and mechanical systems, which proves that the dominant factors (such as geometric angle and rotational speed) tend to explain most variability of the system, almost the same type of observation has also been noted earlier.

4 Conclusion

- Applied load has a large influence on the pressure force distribution in hydrodynamic journal bearings. The peak positive pressure increases with the increase in load between 0 and 0.50 kg, increasing the load carrying capacity of the bearing.
- Rotational speed is also very critical in pressure distribution. As speed rises to 750 RPM, a peak pressure zone shifts to 120º-150º to 120º-180º resulting in better lubrication and hydrodynamic pressure generation.
- The findings of the experiment indicate that distribution of pressure is sensitive to changes in load and speed. A high load changes angular position of peak pressure whereas greater speeds increase the effectiveness of lubrication.
- The highest pressure is found in the converging wedge area (90º -270º) where the lubricant film thickness is the least. Wear, overheating and mechanical failure can be avoided by proper choice of lubricant and working conditions. On the one hand, the maximum values of pressure occur in the range of 120º -150º, and rotational speed influences pressure more than the applied load.
- Angle is identified as a most pronouncing or influencing parameters but speed is found as more influencing parameter when compared to load. The analysis of ANOVA demonstrates that the Angle parameter is the most essential, and then comes Speed and Load, which have statistically significant effects ($p < 0.05$). The high effect sizes prove the model and the soundness of the experimental design.

References:

[1] J. Zhou, “Pressure Distribution Analysis of Hydrodynamic Journal Bearing using Artificial Neural Network,” in *International Conference on Computer and Automation Engineering, 4th (ICCAE 2012)*, 2012. doi: 10.1115/1.859940.paper24.

[2] M. Tauviqirrahman *et al.*, “CFD analysis of hydrodynamic journal bearing with Bingham plastic lubricant considering roughness,” *Cogent Eng*, vol. 10, no. 1, 2023, doi: 10.1080/23311916.2023.2213537.

[3] P. Kumar and A. K. Gupta, “Experimental Investigation on Hydrodynamic Journal Bearing using SAE 10W30 Multi Grade Oil,” *International Journal of Advance Research and Innovation*, vol. 2, no. 1, 2014.

[4] Q. Zhou, Y. Li, and P. Lu, “Studies on thermal effects in aerodynamic foil journal bearings,” 2016. doi: 10.1299/jamdsm.2016jamdsm0011.

[5] S. M. Chun, “Thermohydrodynamic lubrication analysis of high-speed journal bearing considering variable density and variable specific heat,” *Tribol Int*, vol. 37, no. 5, 2004, doi: 10.1016/j.triboint.2003.12.009.

[6] J. Sep, “Three-dimensional hydrodynamic analysis of a journal bearing with a two-component surface layer,” *Tribol Int*, vol. 38, no. 2, 2005, doi: 10.1016/j.triboint.2004.02.004.

[7] J. Bouyer and M. Fillon, “Experimental measurement of the friction torque on hydrodynamic plain journal bearings during start-up,” *Tribol Int*, vol. 44, no. 7–8, 2011, doi: 10.1016/j.triboint.2011.01.008.

[8] N. K. Arakere, H. D. Nelson, and R. L. Rankin, “Hydrodynamic lubrication of finite length rough gas journal bearings,” *Tribology Transactions*, vol. 33, no. 2, 1990, doi: 10.1080/10402009008981948.

[9] I. Rudnieva, Y. Priadko, H. Tonkacheiev, and M. Priadko, “Investigation of the effectiveness of strengthening with FRP applied in metal elements of suspension roof: an analytical approach,” *Strength of Materials and Theory of Structures*, no. 107, 2021.

[10] T. E. Carl, “Paper 19: An Experimental Investigation of a Cylindrical Journal Bearing under Constant and Sinusoidal Loading,” *Proceedings of the Institution of Mechanical Engineers, Conference Proceedings*, vol. 178, no. 14, 1963, doi: 10.1243/pime_conf_1963_178_381_02.

[11] S. Baskar and G. Sriram, “Experimental analysis of hydrodynamic journal bearing under different biolubricants,” in *IEEE-International Conference on Advances in Engineering, Science and Management, ICAESM-2012*, 2012.

[12] D. T. Gethin, “Modelling the thermohydrodynamic behaviour of high speed journal bearings,” *Tribol Int*, vol. 29, no. 7, 1996, doi: 10.1016/0301-679X(96)00004-7.

[13] J. Liu and Y. Mochimaru, “Pressure Distributions Generated along a Self-Acting Fluid-Lubricated Herringbone-Grooved Journal Bearing with Trapezoidal Groove,” *ISRN Tribology*, vol. 2013, 2013.

Kaushal Kumar, Paramvir Yadav,
Deekshant Varshney, Prawar,
Chintan Singh, Subhav Singh

[14] A. Shinde, P. Pawar, P. Shaikh, S. Wangikar, S. Salunkhe, and V. Dhamgaye, "Experimental and Numerical Analysis of Conical Shape Hydrodynamic Journal Bearing with Partial Texturing," in *Procedia Manufacturing*, 2018. doi: 10.1016/j.promfg.2018.02.045.

[15] D. C. Katpatal, A. B. Andhare, and P. M. Padole, "Performance of nano-bio-lubricants, ISO VG46 oil and its blend with Jatropha oil in statically loaded hydrodynamic plain journal bearing," *Proceedings of the Institution of Mechanical Engineers, Part J: Journal of Engineering Tribology*, vol. 234, no. 3, 2020, doi: 10.1177/1350650119864242.

[16] V. K. Sharma, R. C. Singh, and R. Chaudhary, "Study of Starting Friction during the Running of Plain Journal Bearing under Hydrodynamic Lubrication Regime," in *SAE Technical Papers*, 2018.

[17] Andras Z. Szeri, "Fluid film lubrication: theory and design," *Choice Reviews Online*, vol. 36, no. 10, 1999, https://doi.org/10.1017/CBO9780511626401

[18] B. J. Hamrock and D. Dowson, "Ball bearing lubrication. The elastohydrodynamics of elliptical contacts.," 1981, doi: 10.1115/1.3253193.

[19] F. E. Kennedy, "Applied Tribology: Bearing Design and Lubrication," *J Tribol*, vol. 124, no. 2, 2002, doi: 10.1115/1.1432665.

[20] O. Hussain, B. Ahmad, and S. Saleem, "Analysis of tribological behavior of medical-grade UHMW polyethylene under dry and lubricated conditions with human body fluids using Taguchi and GRA techniques," *Journal of Thermoplastic Composite Materials*, vol. 35, no. 11, 2022, doi: 10.1177/0892705720941907.

[21] P. Yadav *et al.*, "Analysis of the performance characteristics of mild steel-based hydrodynamic journal bearings under varying conditions," *Industrial Lubrication and Tribology*, May 2025, doi: 10.1108/ILT-03-2025-0114.

[22] A. Warhurst, "Sustainability indicators and sustainability performance management," *Sustainability Indicators and Sustainability Performance Management*, vol. 43, no. 43, 2002.

[23] M. Li *et al.*, "Research on AFM tip-related nanofabrication of two-dimensional materials," 2023. doi: 10.1515/ntrev-2023-0153.

[24] B. K. Prasad, "Sliding wear behaviour of zinc-based alloyvis-à -vis gray cast iron as influenced by applied load and sliding speed," *Industrial Lubrication and Tribology*, vol. 63, no. 3, 2011, https://doi.org/10.1108/00368791111126581.

Contribution of Individual Authors to the Creation of a Scientific Article (Ghostwriting Policy)

The authors equally contributed in the present research, at all stages from the formulation of the problem to the final findings and solution.

Sources of Funding for Research Presented in a Scientific Article or Scientific Article Itself

No funding was received for conducting this study.

Conflict of Interest

The authors have no conflicts of interest to declare that are relevant to the content of this article.

Kaushal Kumar, Paramvir Yadav,
Deekshant Varshney, Prawar,
Chintan Singh, Subhav Singh

APPENDIX

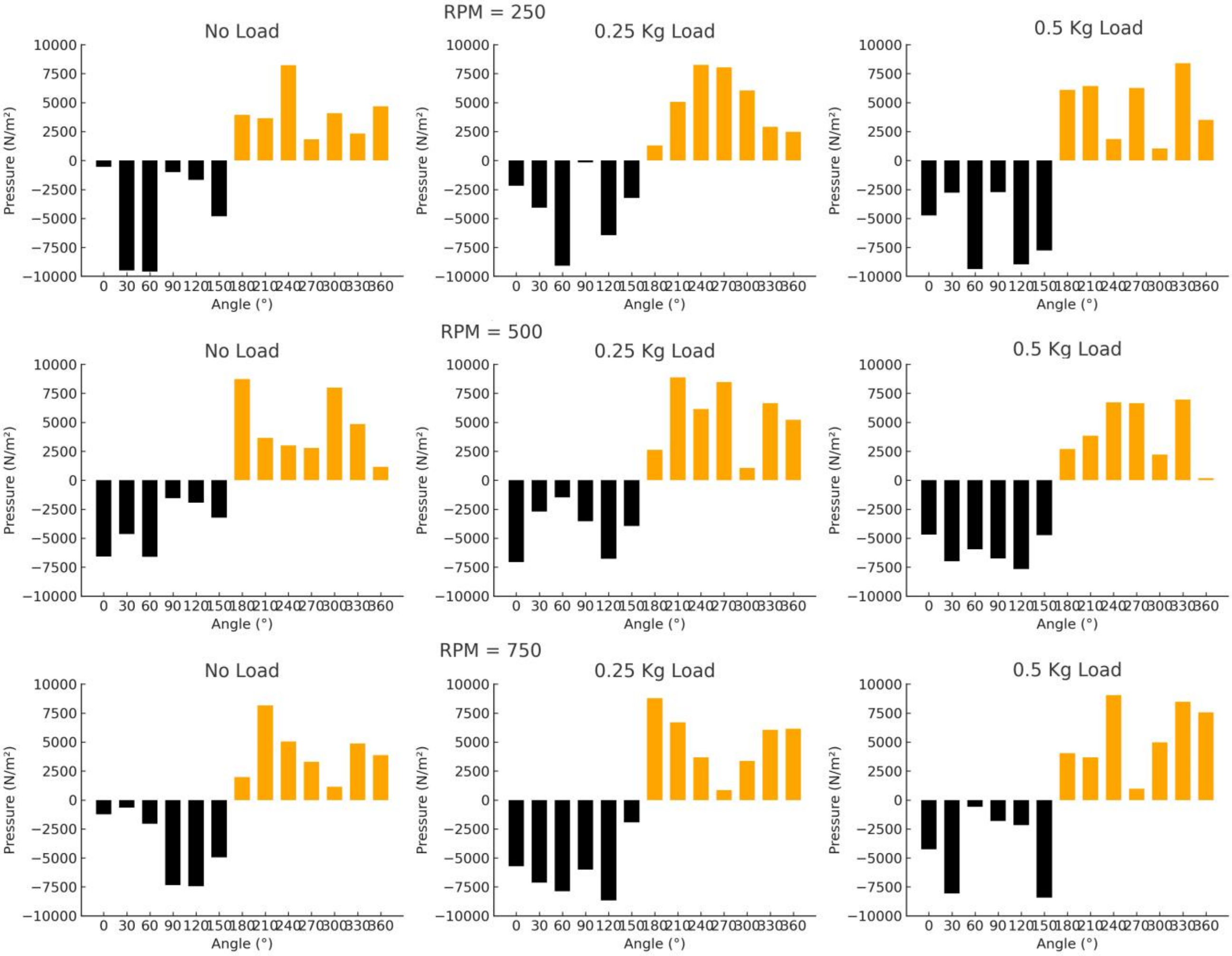

Fig. 3: Circumferential pressure distribution at varying load conditions for constant speed
Source: created by the authors

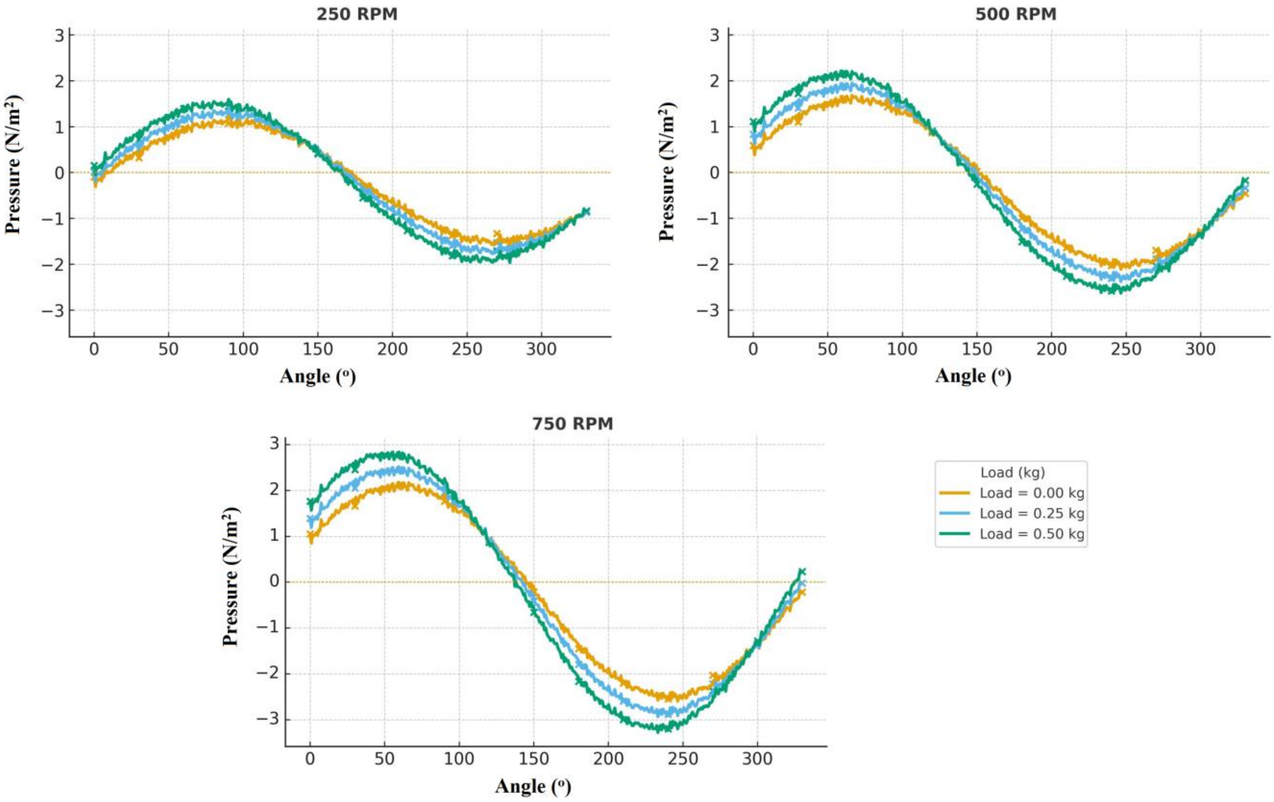

Fig. 4: Variation in pressure distribution with change in load at constant speed

Source: created by the authors

Kaushal Kumar, Paramvir Yadav,
Deekshant Varshney, Prawar,
Chintan Singh, Subhav Singh

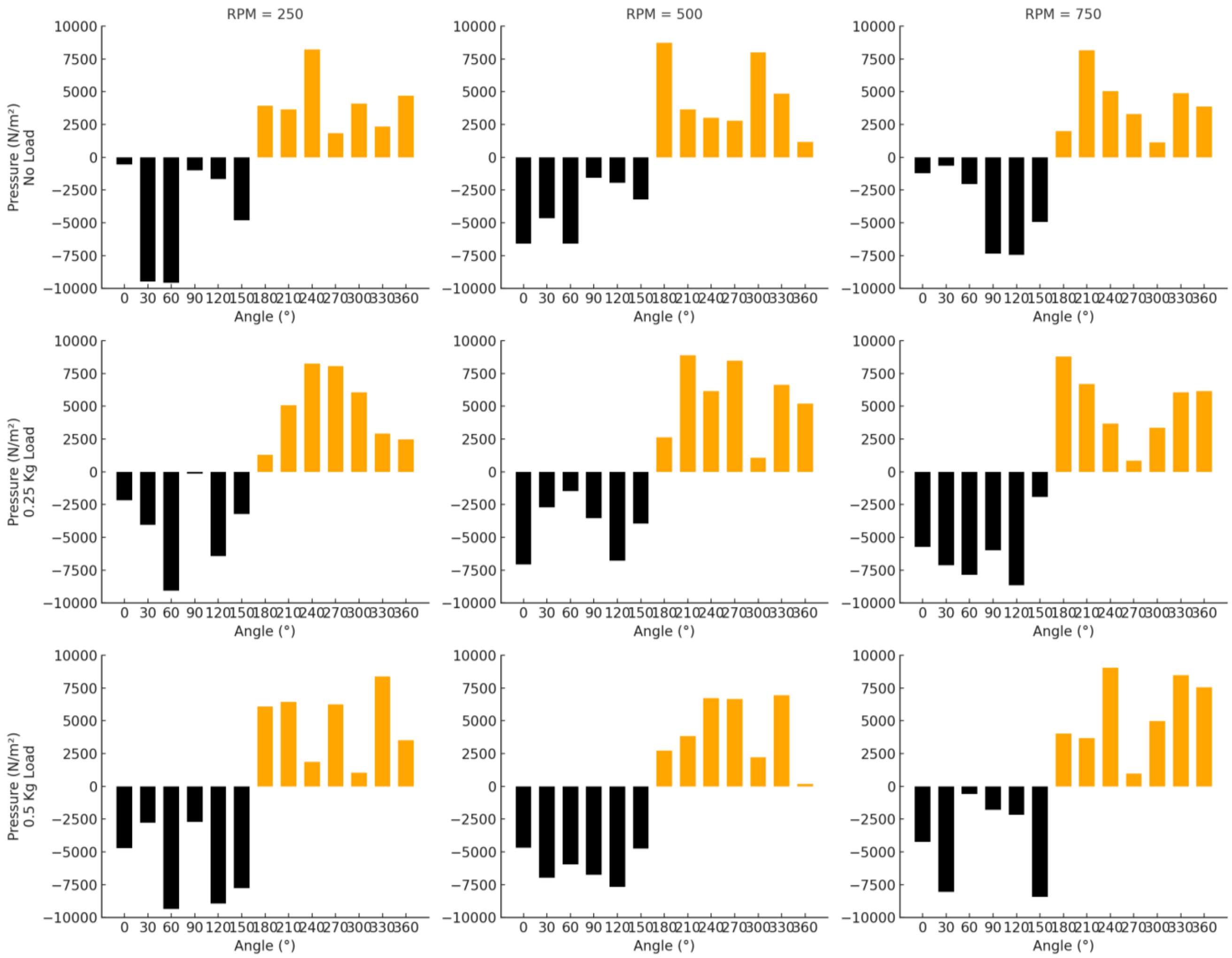

Fig. 5: Circumferential pressure distribution at varying speed for constant load
Source: created by the authors

Kaushal Kumar, Paramvir Yadav,
Deekshant Varshney, Prawar,
Chintan Singh, Subhav Singh

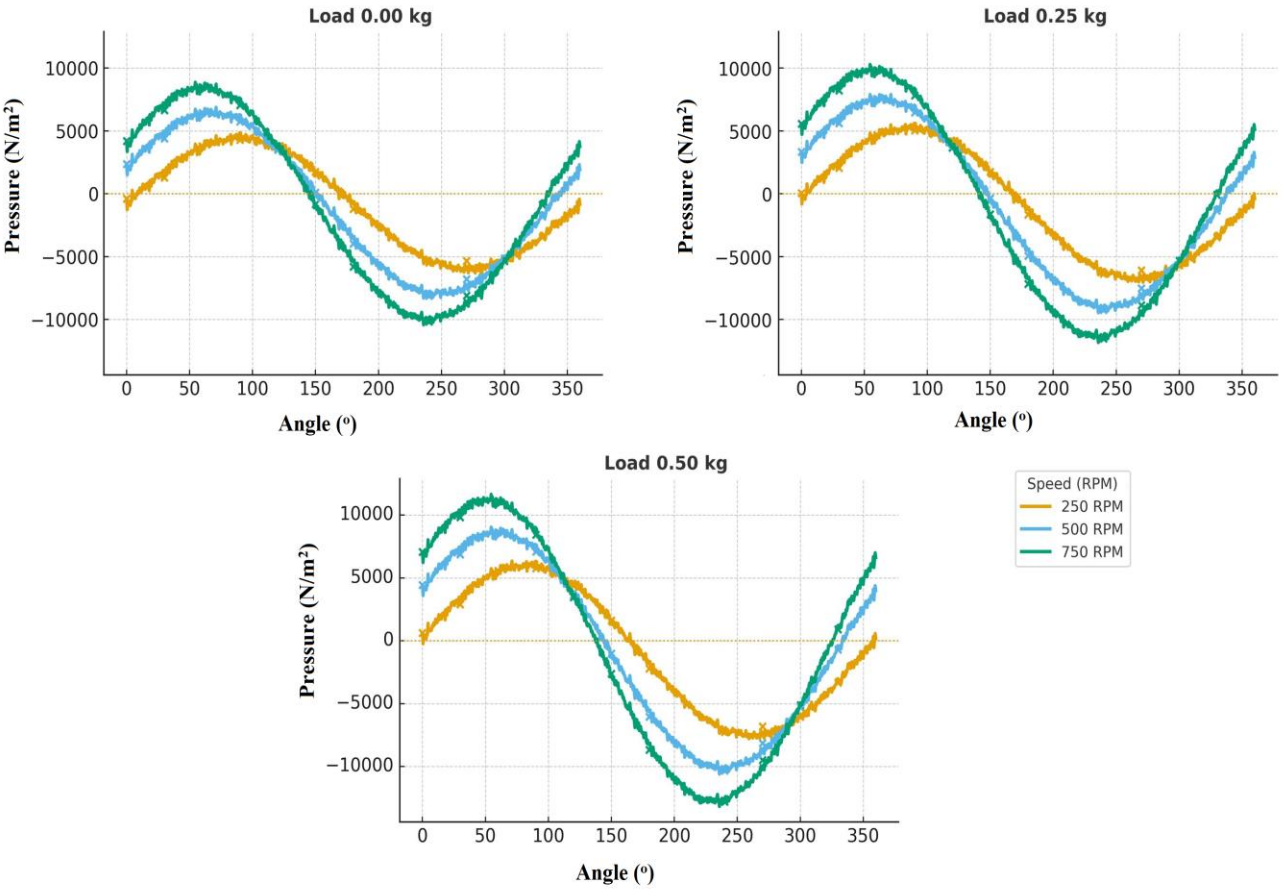

Fig. 6: Variation in pressure distribution with change in speed at constant load

Source: created by the authors